Title

Hypoxia-ischemia modifies postsynaptic GluN2B-containing NMDA receptor complexes in the neonatal mouse brain

Journal

Experimental Neurology, 299(Pt A)

ISSN

0014-4886

Authors

Lu, Fuxin
Shao, Guo
Wang, Yongqiang
et al.

Publication Date

2018

DOI

10.1016/j.expneurol.2017.10.005

Peer reviewed

Experimental Neurology 299 (2018) 65–74

Contents lists available at ScienceDirect

Experimental Neurology

journal homepage: www.elsevier.com/locate/yexnr

Research Paper

Hypoxia-ischemia modifies postsynaptic GluN2B-containing NMDA receptor complexes in the neonatal mouse brain

Fuxin Lu[a], Guo Shao[b], Yongqiang Wang[c,d], Shenheng Guan[e], Alma L. Burlingame[e], Xuemei Liu[f], Xiao Liang[f], Renatta Knox[g], Donna M. Ferriero[a,h], Xiangning Jiang[a,*]

[a] Department of Pediatrics, University of California San Francisco, CA, USA
[b] Inner Mongolia Key Laboratory of Hypoxic Translational Medicine, Baotou Medical College, Baotou, China
[c] Department of Cellular & Molecular Pharmacology, University of California San Francisco, CA, USA
[d] Howard Hughes Medical Institute, University of California, San Francisco, CA, USA
[e] Department of Pharmaceutical Chemistry, University of California San Francisco, CA, USA
[f] Central Laboratory, Dongfang Hospital, Beijing University of Chinese Medicine, Beijing, China
[g] Department of Pediatrics, Weill Cornell Medical College, New York, NY, USA
[h] Department of Neurology, University of California San Francisco, CA, USA

ARTICLE INFO

Keywords:
Brain
Development
Hypoxia/ischemia
NMDA receptors
Proteomics

ABSTRACT

The *N*-methyl-D-aspartate-type glutamate receptor (NMDAR)-associated multiprotein complexes are indispensable for synaptic plasticity and cognitive functions. While purification and proteomic analyses of these signaling complexes have been performed in adult rodent and human brain, much less is known about the protein composition of NMDAR complexes in the developing brain and their modifications by neonatal hypoxic-ischemic (HI) brain injury. In this study, the postsynaptic density proteins were prepared from postnatal day 9 naïve, sham-operated and HI-injured mouse cortex. The GluN2B-containing NMDAR complexes were purified by immunoprecipitation with a mouse GluN2B antibody and subjected to mass spectrometry analysis for determination of the GluN2B binding partners. A total of 71 proteins of different functional categories were identified from the naïve animals as native GluN2B-interacting partners in the developing mouse brain. Neonatal HI reshaped the postsynaptic GluN2B interactome by recruiting new proteins, including multiple kinases, into the complexes; and modifying the existing associations within 1 h of reperfusion. The early responses of postsynaptic NMDAR complexes and their related signaling networks may contribute to molecular processes leading to cell survival or death, brain damage and/or neurological disorders in term infants with neonatal encephalopathy.

1. Introduction

The *N*-methyl-D-aspartate-type glutamate receptors (NMDARs) are essential for the maturation of glutamatergic synapses (Paoletti et al., 2013) and neuronal survival in the developing brain (Hansen et al., 2004), however, over-activation of the receptors contributes to cell death in brain hypoxia-ischemia (HI), stroke or trauma. The NMDARs contain two obligate GluN1 subunits and typically two regulatory GluN2 subunits, GluN2A-2D. The GluN2B is highly expressed prenatally and at early postnatal age (Monyer et al., 1994; Wenzel et al., 1997), suggesting its importance in brain development, neuronal migration, synaptic plasticity and circuit formation (Hall et al., 2007; Kutsuwada et al., 1996; Mancini and Atchison, 2007; Ohno et al., 2010; Tarnok et al., 2008; Wang et al., 2011). In fact, mutations in the human GRIN2B gene encoding GluN2B are implicated in various neurodevelopmental disorders, especially intellectual disability (ID), developmental delay (DD), autism, epilepsy and/or seizure, and other behavioral issues (Burnashev and Szepetowski, 2015; Hu et al., 2016).

Besides the inotropic property as a calcium channel, the NMDARs exert metabotropic function using their cytoplasmic C-terminal domain (CTD) to assemble multi-protein complexes at postsynaptic density (PSD) that drive intracellular signaling transduction (Fan et al., 2014). Mice expressing truncated GluN2A or GluN2C CTD show impaired synaptic plasticity or motor coordination, while expressing truncated GluN2B CTD die prenatally. These phenotypes may reflect defective intracellular signaling (Sprengel et al., 1998). Proteomic analyses of human cortex PSD demonstrated a correlation of protein abundance in the NMDAR complex between mouse and human (Bayes et al., 2012).

* Corresponding author at: Department of Pediatrics, University of California, San Francisco 675 Nelson Rising Lane Room 494, San Francisco, CA 94158, USA.
E-mail address: xiangning.jiang@ucsf.edu (X. Jiang).

http://dx.doi.org/10.1016/j.expneurol.2017.10.005
Received 23 May 2017; Received in revised form 9 September 2017; Accepted 5 October 2017
Available online 06 October 2017

These complexes, and the membrane-associated guanylate kinases (MAGUK)-associated complexes, contain proteins that contribute to human cognitive intelligence (Hill et al., 2014), and are associated with a wide range of human brain diseases, including mental, behavioral disorders & ID that present in patients with GRIN2B defects (Bayes et al., 2014; Pocklington et al., 2006). These findings emphasize the importance of characterizing the major synaptic protein networks for clarifying their significance in disease mechanisms and for identifying synaptic therapeutic targets.

The size and composition of NMDAR complexes are developmentally regulated (Frank et al., 2016). Therefore, their responses to neuronal activity, and to excessive glutamate release in pathological conditions could be age-dependent. Characterization of the NMDAR complexes in the developing brain is imperative for understanding the molecular basis of structural and functional plasticity during synapse maturation. Likewise, how injury paradigms during rapid brain growth reshape the synaptic complexes and related signaling; whether the modifications at the synaptic level contribute to long term neurological or psychiatric outcomes are critical to be clarified.

Peptide-based affinity purification followed by mass spectrometry (MS) analysis has identified > 100 proteins in the NMDAR or MAGUK complexes in adult mouse brain (Collins et al., 2006; Husi and Grant, 2001; Husi et al., 2000). Unfortunately, investigations of these complexes during brain development and after brain injury are lacking. Here we use a mouse model of neonatal HI to mimic human neonatal encephalopathy (NE), a clinically defined neurological disorder with HI as a common contributor (Millar et al., 2017). Survivors of moderate to severe NE often present with brain damage leading to neuromotor (cerebral palsy, epilepsy) and cognitive (mental retardation, learning disability) impairments (de Vries and Jongmans, 2010; Pappas et al., 2015; Perez et al., 2013; van Handel et al., 2007). Based on the fact that GluN2B is predominant in the immature brain whose CTD promotes pro-death NMDAR signaling under excitotoxicity or ischemia (Martel et al., 2012; Shu et al., 2014; Sun et al., 2015), and the implication of GluN2B in cognitive/behavioral deficits in brain development, we hypothesized that HI modifies the GluN2B-containing NMDAR complexes and the associated signaling pathways in the neonatal brain.

Using immunoprecipitation combined with MS-based proteomic analysis, we identified 71 native GluN2B binding partners from the naïve postnatal day 9 (P9) mouse cortex. Within 1 h after neonatal HI, 37 proteins were recruited to the complexes including multiple kinases that could phosphorylate the GluN2B subunit at different sites. Four novel proteins were validated to interact with GluN2B after HI: IQ motif and SEC7 domain-containing protein 1 (IQSEC1 or BRAG2); eukaryotic translation elongation factor 1 (Eef1α1); Tetratricopeptide Repeat, Ankyrin Repeat And Coiled-Coil Containing 2 (TANC2) and Neuron navigator 1 (NAV1). In addition, HI reorganized the GluN2B complexes by up- or down- regulating its interactions with various PSD proteins. The post-HI GluN2B complexes showed a high enrichment in molecules involved in neurological diseases that may be associated with clinical NE manifestation and neurological outcomes.

2. Materials and methods

All animal experiments were approved by the University of California San Francisco (UCSF) institutional animal care and use committee. C57BL/6 mice (Simonsen Laboratories) with litters were allowed food and water ad libitum. Both sexes were used for these studies at P9.

2.1. Neonatal brain hypoxia-ischemia

Neonatal HI was performed as previously described using the Vannucci model (Rice et al., 1981). At P9, pups were anesthetized with isoflurane (2–3% isoflurane/balance oxygen) and the left common carotid artery was electrocauterized. The animals were recovered for 1 h with their dam and then exposed to 60 min of hypoxia in a humidified chamber at 37 °C with 10% oxygen/balance nitrogen. Sham-operated control animals received isoflurane anesthesia and exposure of the left common carotid artery without ligation or hypoxia. HI and sham animals were returned to their dams until they were euthanized at 15 min, 1 h, 6 h and 24 h after the procedure for different experiments.

2.2. PSD sample preparation

Purification of PSD-associated synaptic proteins was carried out as described using a subcellular fractionation approach followed by extraction with Triton X-100 (Jiang et al., 2011; Knox et al., 2013). Cortical tissue was homogenized in ice-cold 0.32 M sucrose buffer and centrifuged at 1000 × *g* for 10 min. The resulting supernatant was spun at 10,000 × *g* for 15 min to yield a pellet as crude membrane fraction (P2). The P2 was resuspended in 120 µl sucrose buffer, mixed with 8 volumes of 0.5% Triton X-100 buffer and homogenized again with 30 pulses of a glass pestle followed by rotation at 4 °C for 30 min. After Triton extraction, the samples were spun at 32,000 × g for 30 min in a TL-100 tabletop ultracentrifuge (Beckman). The resultant pellet containing Triton X-insoluble PSD proteins were dissolved in TE buffer (100 mM Tris-HCl, 10 mM EDTA) with 0.5% SDS and stored at − 80 °C until use. Protein concentration was determined by the bicinchoninic acid method (Pierce). The purity of PSD was verified by Western blots as described (Jiang et al., 2011).

2.3. Immunoprecipitation (IP) and in gel digestion

The GluN2B protein complexes were purified from PSD samples by immunoprecipitation with a mouse GluN2B monoclonal antibody (MBS800075, Lot# 1003, MyBioSource Inc. San Diego, CA). Briefly, 25 µg PSD protein was diluted with 1% NP40 buffer and pre-cleared with 25 µl Protein G-agarose beads (#15920-010, Invitrogen, Waltham, MA) for 30 min at 4 °C. The samples were then incubated overnight with 6.25 µg GluN2B antibody or 6.25 µg mouse IgG2b (#401202, BioLegend, San Diego, CA) as a negative control with slow rotation. The next day, 50 µl of protein G-agarose beads was added and the sample mixtures were rotated for another 2 h. After centrifugation, the beads were washed 3 times with NP40 buffer and boiled for 10 mins with 30 µL of 2x LDS sample buffer (Invitrogen). The GluN2B binding proteins in the supernatant were then separated by NuPAGE Novex 4–12% Bis-Tris Gels for Western blotting (see below) to validate protein interactions, or stained with Imperial protein stain (#24615, Thermo Scientific, Waltham, MA) for in gel digestion followed by LC-MS/MS analysis (Shao et al., 2017). Lanes were sliced into 0.5–1 mm^3 small pieces and placed into low-binding eppendorf tubes for destaining, dehydration, reduction and alkylation followed by digestion with combined trypsin (sequencing grade, Promega) and lysyl endopeptidase C (Lys-C, mass spectrometry grade, Wako) at the ratio of enzyme: protein of 1:25 in mass. After incubation at 37 °C for 16 h, the digested peptides were extracted and desalted with C18 solid phase extraction tip (10 µl bed C18 ZipTip, Pierce) and then eluted with two sequential 10ul aliquots of 50% acetonitrile in 0.1% trifluoroacetic acid. The combined elute was dried in Speed Vac and resuspended in 0.1% formic acid/2% acetonitrile for the subsequent MS analysis.

2.4. LC-MS/MS analysis and protein identification

The peptides were analyzed by LC-MS/MS on LTQ Orbitrap mass spectrometer (ThermoFisher Scientific, San Jose, CA) equipped with a Waters NanoAcquity LC system (Milford, MA) at UCSF Mass Spectrometry Facility (Shao et al., 2017). Peptides were separated on an Easy-Spray column (Thermo, PepMap, C18, 3 µm, 100 Å, 75 µm × 15 cm) using a linear gradient from 2% solvent A (0.1% formic acid in water) to 25% solvent B (0.1% formic acid in acetonitrile) at 300 nL/min over 47 min. MS precursor spectra were measured

in the Orbitrap from 300 to 2000 *m/z* at 30,000 resolving power, top six precursor ions were selected and dissociated by collision-induced dissociation (CID) for MS/MS. The MS/MS data were searched against mouse protein sequences in the SwissProt database (downloaded from Uniprot on 2015.10.12) using MSGF + search engine (Kim and Pevzner, 2014) with a concatenated database consisting of normal and randomized decoy databases. The false discovery rates for peptide identification were estimated to be 1.2%, corresponding to maximum expectation value of 0.102. Parent/precursor mass tolerance and fragment mass tolerance were 20 ppm and 0.6 Da, respectively. Constant modification of carbamidomethylation on cysteine (C) and variable modifications of deamidation of N-terminal glutamine, initial protein methionine loss with or without N-terminal acetylation were employed.

2.5. Semi-quantification of GluN2B protein interactions using spectral counting

A semi-quantitative analysis was performed using spectral counting, which relies on the number of peptides (peptide count) identified from a given protein. This simple label-free quantification technique is based on the observation that the more abundant a protein is, the more peptides can be identified from it. It provides a tool for rapid screening and broad estimation of relative protein amount between samples (Old et al., 2005). To estimate the relative level of protein interaction with GluN2B, the mean peptide count of individual protein from triplicate analysis (three repeated LC/MS/MS analysis of the same sample) was normalized to that of GluN2B in each specific MS experiment. The proteins that appeared in three MS experiments were selected and reported with standard deviations (SD) and coefficient of variation (%CV). The mean fold changes of HI over sham values were used to represent the up- or down-regulation of GluN2B interactions for each protein after HI. Calculation of fold change was made following Ingenuity Pathway Analysis (IPA, Qiagen, Redwood, CA), the bioinformatics tool that we utilized for functional analysis. If the association increased after HI, use values of (HI/sham), and if the association decreased after HI, use − 1(sham/HI).

2.6. Western blotting

For Western blot analysis, an equal amount of PSD protein samples (5 μg) or equal volume of supernatant from GluN2B IP experiments was applied to 4–12% Bis-Tris SDS polyacrylamide gel electrophoresis and transferred to polyvinylidene difluoride (PVDF) membrane. The blots were probed with the primary antibodies (listed in Supplemental Table S2) overnight at 4 °C. Appropriate secondary horseradish peroxidase-conjugated antibodies (Santa Cruz Biotechnology Inc.) were used, and signal was visualized with enhanced chemiluminescence (Amersham, GE Healthcare). Image J software was used to measure the mean optical densities (OD) and areas of protein signal on radiographic film after scanning.

2.7. Primary cortical neuronal culture and immunofluorescent staining

Primary neuronal cultures were prepared from embryonic day 16 mouse cortices as described previously (Jiang et al., 2004) and used on day in vitro (DIV) 10 for double immunofluorescent staining to determine co-localization of GluN2B with TANC2 or NAV1. Briefly, the cultures were washed and fixed with 4% paraformaldehyde/4% sucrose in PBS for 12 min on ice followed by 100% methanol for 10 min at − 20 °C. Cells were permeabilized with 0.1% Triton -X100 in PBS for 10 min. After blocking with 3% goat serum in PBS for 1 h, the cells were incubated overnight with primary antibodies diluted in blocking buffer (rabbit anti-GluN2B: #4212 from Cell Signaling Technology, paired with mouse anti-TANC2: sc-515710; or mouse anti-NAV1: sc-398641 from Santa Cruz Biotechnology). After washing three times in PBS and incubation with secondary antibodies (Alexa 488-conjugated goat anti-mouse IgG and Alexa 568-conjugated goat anti-rabbit IgG) at room temperature for 1 h, the cultures were counterstained with DAPI. Images were captured with Zeiss Axiovert microscope.

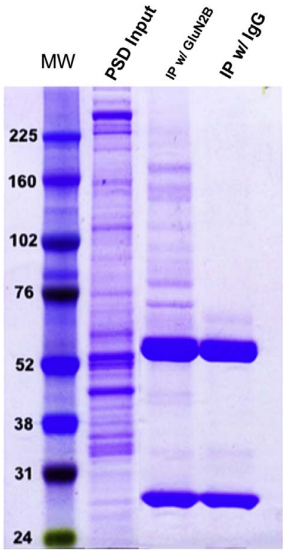

Fig. 1. Coomassie blue protein staining of SDS-PAGE (4–12%) for immunoprecipitation (IP) with GluN2B antibody or with normal mouse IgG (as negative control) from P9 mouse cortex PSD fractions (25 μg). Multiple specific GluN2B binding proteins were visualized. The two bands in IgG lane were IgG heavy chain (approximately 50 KDa) and light chain (25 KDa). PSD input was 2.5 μg. MW: protein molecular weight marker. (For interpretation of the references to colour in this figure legend, the reader is referred to the web version of this article.)

2.8. Functional analysis with Ingenuity Pathway Analysis (IPA)

To evaluate whether the changes in GluN2B interactions with other PSD proteins at early stage (1 h) after HI are associated with any forms of biological processes or diseases, we interrogated the data with IPA. A list of proteins identified from MS experiments that were newly recruited to the complexes after HI and proteins with differential levels of interactions to GluN2B after HI was generated. The list containing the protein ID (UniProt Accession number) along with the values of mean fold changes of HI over sham was uploaded to the software for a core analysis. IPA identifies genes associated with a list of relevant functions and diseases using a constantly updated knowledge base, and the list is ranked based on the significance of the biological functions. Direct and indirect relationships were considered for the analysis. We interrogated specifically the function and neurological disease annotation in IPA and the top 10 for these two categories were reported.

2.9. Statistical analysis

GluN2B-ineracting proteins detected by MS experiments were semi-quantified using spectral counting from triplicate MS run of 3 sets of samples for each group. As mentioned above, the relative levels of the association of each individual protein with GluN2B were calculated. The differences between HI and sham animals are presented as mean fold change of HI/sham, along with SD and %CV. For Western Blotting, the optical densities of protein bands were presented as mean ± SD and were evaluated statistically using SAS Wilcoxon-Mann-Whitney test. Differences were considered significant at $p < 0.05$.

Table 1
Proteins recruited to the GluN2B complexes early after neonatal HI (1 h) in P9 mouse cortex.

Protein			Mean peptide counts normalized to GluN2B	SD	%CV
Acc#	Gene	Protein name			
Q8CH77	Nav1	Neuron navigator 1	0.653	0.137	21.063
Q8R0S2	Iqsec1	IQ motif and SEC7 domain-containing protein 1	0.430	0.250	58.140
A2A690	Tanc2	Protein TANC2	0.382	0.016	4.167
P10126	Eef1a1	Elongation factor 1-alpha 1	0.346	0.104	30.026
Q9JLM8	Dclk1	Serine/threonine-protein kinase DCLK1	0.325	0.007	2.176
Q99NE5	Rims1	Regulating synaptic membrane exocytosis protein 1	0.277	0.025	9.034
P63318	Prkcg	Protein kinase C gamma type	0.256	0.084	32.748
Q3UHL1	Camkv	CaM kinase-like vesicle-associated protein	0.225	0.078	34.570
P46460	Nsf	Vesicle-fusing ATPase	0.219	0.031	14.335
Q5DTT2	Psd	PH and SEC7 domain-containing protein 1	0.217	0.097	44.841
Q80YF9	Arhgap33	Rho GTPase-activating protein 33	0.208	0.059	28.284
Q923T9	Camk2g	Calcium/calmodulin-dependent protein kinase type II subunit gamma	0.206	0.100	48.614
Q8K341	Atat1	Alpha-tubulin *N*-acetyltransferase 1	0.200	0.031	15.402
P68404	Prkcb	Protein kinase C beta type	0.180	0.020	11.111
F8VPU2	Farp1	FERM, RhoGEF and pleckstrin domain-containing protein 1	0.182	0.005	2.571
Q3UHD9	Agap2	Arf-GAP with GTPase, ANK repeat and PH domain-containing protein 2	0.163	0.073	44.841
Q4KUS2	Unc13a	Protein unc-13 homolog A	0.163	0.073	44.841
Q9QUG9	Rasgrp2	RAS guanyl-releasing protein 2	0.146	0.029	20.203
Q5XJV6	Lmtk3	Serine/threonine-protein kinase LMTK3	0.146	0.004	2.571
Q8K4P8	Hecw1	E3 ubiquitin-protein ligase HECW1	0.146	0.004	2.571
O35927	Ctnnd2	Catenin delta-2	0.142	0.050	35.060
Q9R1L5	Mast1	Microtubule-associated serine/threonine-protein kinase 1	0.126	0.074	58.494
Q62417	Sorbs1	Sorbin and SH3 domain-containing protein 1	0.108	0.049	44.841
Q16539	MAPK14	Mitogen-activated protein kinase 14	0.110	0.040	36.364
Q80YA9	Cnksr2	Connector enhancer of kinase suppressor of ras 2	0.108	0.049	44.841
Q8VHH5	Agap3	Arf-GAP with GTPase, ANK repeat and PH domain-containing protein 3	0.082	0.011	13.169
Q6PH08	Erc2	ERC protein 2	0.075	0.028	37.298
Q6PHZ2	Camk2d	Calcium/calmodulin-dependent protein kinase type II subunit delta	0.075	0.025	33.748
A2CG49	Kalrn	Kalirin	0.073	0.002	2.571
P20444	Prkca	Protein kinase C alpha type	0.073	0.002	2.571
Q80ZF8	Adgrb3	Adhesion G protein-coupled receptor B3	0.073	0.002	2.571
Q68FH0	Pkp4	Plakophilin-4	0.058	0.019	32.934
P59281	Arhgap39	Rho GTPase-activating protein 39	0.054	0.024	44.841
P68181	Prkacb	cAMP-dependent protein kinase catalytic subunit beta	0.054	0.024	44.841
Q69ZH9	Arhgap23	Rho GTPase-activating protein 23	0.036	0.001	2.571
Q9CX86	Hnrnpa0	Heterogeneous nuclear ribonucleoprotein A0	0.036	0.001	2.571
Q9Z1W9	Stk39	STE20/SPS1-related proline-alanine-rich protein kinase	0.041	0.001	3.449

The identified proteins are reported with their UniProt accession number (Acc#), gene and protein name, relative level of binding to GluN2B (mean peptide counts normalized to GluN2B) with the standard deviation (SD) and coefficient of variation (%CV). The interaction of GluN2B with the underlined proteins was validated by co-IP experiments.

3. Results

3.1. Protein components of native postsynaptic GluN2B complexes in the neonatal mouse brain

Postsynaptic GluN2B complexes were purified from PSD fractions by IP with a mouse GluN2B monoclonal antibody that targets the N-terminus of GluN2B (amino acids 20–127). Selection of this antibody was to avoid interferences with the GluN2B interactions that are assembled on its C-terminus. The antibody successfully pulled down numerous GluN2B binding partners that were visualized in Coomassie blue - stained SDS-PAGE gel (Fig. 1). These bindings were specific to GluN2B as no proteins were precipitated with normal mouse IgG as a negative control. After gel slicing, in-gel digestion and MS analysis/database search, a total of 71 proteins were identified, which were classified into different functional groups based on their published biological functions (Supplemental Table S1). The identified proteins were reported with their name, UniProt accession number, gene name, the number of peptides corresponding to the protein, the percent sequence coverage for the protein, and the best expectation values for the most confident peptide identification for each protein. Similar to reported composition of NMDAR complexes in adult brain (Collins et al., 2006; Husi et al., 2000), main GluN2B-assocaited proteins are scaffold and adaptor proteins (15 proteins) including the MAGUK family members and their interacting proteins, as well as the cytoskeleton and cell adhesion proteins (20 proteins). GluN1, a mandatory NMDAR subunit, was found in the complexes as expected. These interactions enable the NMDARs to be anchored on the postsynaptic membrane and crosslink with PSD backbone structure proteins. Three kinases (CaMKIIα, CaMKIIβ, Src) and SRC kinase signaling inhibitor 1 (SNIP) were detected, while no phosphatases were identified.

3.2. Novel GluN2B interactions induced by neonatal HI

To investigate the modification of the GluN2B complexes following neonatal HI and whether novel GluN2B connections are activated, the protein list of complexes prepared from HI-injured cortex at 1 h after HI was compared to that from sham-operated animals to exclude the effects of anesthesia. There were no differences in the composition or expression of NMDAR complex components in the sham compared to that of the naïve animals. Proteins that appeared only after HI, but not in sham were considered as novel GluN2B interactions triggered by neonatal HI (Table 1). Mean peptide counts of individual protein was normalized to that of GluN2B in each experiment to represent the relative levels of binding to GluN2B. A total of 37 proteins were identified among which the interactions of GluN2B with 8 proteins were validated by co-IP experiments (underlined in Table 1). The top 4 proteins are neuron navigator 1 (NAV1), a microtubule-associated protein involved in neuronal migration (Martinez-Lopez et al., 2005); IQ motif and SEC7 domain-containing protein 1 (Iqsec1 or BRAG2), a guanine-nucleotide exchange factor (GEF) for the small GTPase Arf6 (Um, 2017); Protein TANC2 (Tanc2), a scaffold/adaptor protein binding to various PSD

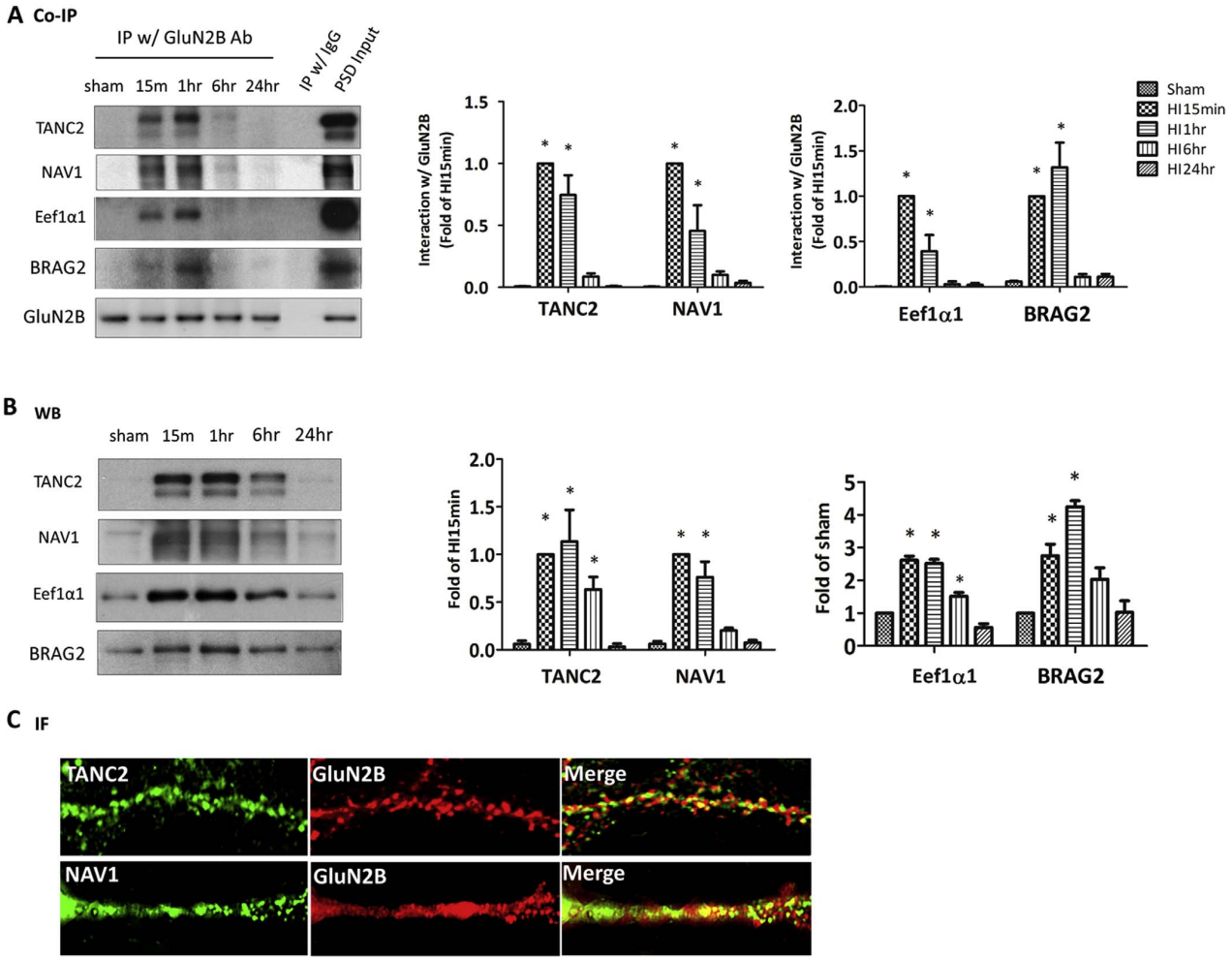

Fig. 2. Novel GluN2B interactions induced by neonatal HI. (A) Co-IP with GluN2B antibody (Ab) showed the interactions of four proteins (labeled on the left side of the blots) with GluN2B after HI that peaked at 15 min or 1 h of reperfusion. IP with mouse IgG served as negative control. Quantification of the protein interactions was shown on the right. The levels of interaction are expressed as the OD ratio of co-IP'd protein (TANC2, NAV1, Eef1α1 or BRAG2) to GluN2B and then normalized to the values of HI 15 min. (* $p < 0.05$ vs. sham, $n = 4$) (B) Western blotting (WB) showed the protein expression of TANC2, NAV1, Eef1α1 and BRAG2 in sham and HI-injured animals. Quantification of the protein levels was shown on the right. Expression of TANC2 and NAV1 was normalized to the values of HI 15 min; expression of Eef1α1 and BRAG2 was normalized to the sham values (* $p < 0.05$ vs. sham, $n = 4$). (C) Images of double immunofluorescent (IF) staining of TANC2 (green in the upper panel), NAV1 (green in the bottom panel) and GluN2B (red). The merged images showed the distribution of TANC2 and NAV1 puncta along the dendrites that partly overlapped with GluN2B ($n = 3$). (For interpretation of the references to colour in this figure legend, the reader is referred to the web version of this article.)

proteins including PSD95 (Suzuki et al., 2005); and Elongation factor 1-alpha 1(Eef1α1), which functions in protein translation (Giustetto et al., 2003). Straight Western blotting experiments were performed in parallel to examine whether these four proteins are present in the PSD and their regulation by neonatal HI (Fig. 2B). Low levels of all four proteins were detected at PSD in sham P9 mouse cortex. Significant translocation of these proteins to the PSDs was observed early after HI that peaked at 15 min and 1 h ($p < 0.05$ vs sham, $n = 4$). Similarly, interactions of GluN2B with these four proteins peaked at 15 min and 1 h, and diminished within 6 h or 24 h after HI (Fig. 2A, $n = 4$). The bindings with GluN2B were specific as no protein was precipitated when using IgG instead of the antibody for co-IP experiments. TANC2, BRAG2 and Eef1α1 have been previously reported to reside at PSD and overlap with PSD95 at spines in cultured neurons (Cho et al., 2004; Elagabani et al., 2016; Han et al., 2010; Suzuki et al., 2005). We examined the localization of TANC2 and NAV1 with GluN2B on dendritic spines in DIV10 primary cortical neurons (Fig. 2C). The distribution of the TANC2 and NAV1 puncta along the dendrites appeared to be partly overlapped with GluN2B, but not completely matched. Although co-localization does not suggest protein interactions, it confirmed their presence on spines and the availability for binding.

3.3. Increased protein kinase-GluN2B interactions early after HI

Semi-quantification for protein interactions with GluN2B was made and compared between sham and injured animals to determine whether the associations are altered (up- and down-regulated) after HI. Top ten proteins with the greatest increase or decrease in GluN2B interaction were reported (Table 2). It was not surprising that HI induced interaction of multiple protein kinases with GluN2B including the 12 proteins listed in Table 1: conventional protein kinase C α, β, γ; CaMKII gamma, delta; CaM kinase-like vesicle-associated protein (CaMKV); PKA subunit beta; serine/threonine protein kinase DCLK1, LMTK3; mitogen-activated protein kinase 14 (p38α), microtubule-associated serine/threonine-protein kinase 1 (MAST1) and STE20/SPS1-related proline-alanine-rich protein kinase (stk39). The interactions between GluN2B and its three native kinase partners, CaMKIIα, β and Src, were also increased (Table 2). SNIP, a negative regulator of Src that is

Table 2
Proteins with differential GluN2B interactions early after neonatal HI (1 h) in P9 mouse cortex.

Top ten proteins with increased GluN2B interactions

Acc#	Gene	Protein name	Fold change (HI/sham)	SD	%CV
P28652	Camk2b	Calcium/calmodulin-dependent protein kinase type II subunit beta	14.040	0.806	5.741
P11798	Camk2a	Calcium/calmodulin-dependent protein kinase type II subunit alpha	8.534	1.166	13.662
P18872	Gnao1	Guanine nucleotide-binding protein G(o) subunit alpha	6.000	0.000	0.000
P05480	Src	Neuronal proto-oncogene tyrosine-protein kinase Src	5.330	2.410	45.216
P68369	Tuba1a	Tubulin alpha-1A chain	4.542	1.002	22.057
B1AQX9	Srcin1	SRC kinase-signaling inhibitor 1 (SNIP)	4.054	0.234	5.775
Q9QYX7	Pclo	Protein piccolo	4.000	0.000	0.000
B1AZP2	Dlgap4	Disks large-associated protein 4	3.000	0.000	0.000
P0CG49	Ubb	Polyubiquitin-B	2.924	0.899	30.732
O88737	Bsn	Protein bassoon	2.667	1.300	48.744

Top ten proteins with decreased GluN2B interactions

Acc#	Gene	Protein name	Fold change (HI/sham)	SD	%CV
D3YZU1	Shank1	SH3 and multiple ankyrin repeat domains protein 1	− 4.100	0.048	19.651
Q9Z2Y3	Homer1	Homer protein homolog 1	− 2.090	0.272	56.864
Q91XM9	Dlg2	Disks large homolog 2 (PSD93)	− 1.910	0.008	1.443
P70175	Dlg3	Disks large homolog 3 (SAP102)	− 1.840	0.174	32.102
P35438	Grin1	Glutamate receptor ionotropic, NMDA 1	− 1.580	0.116	18.377
Q62108	Dlg4	Disks large homolog 4 (PSD95)	− 1.560	0.212	33.175
Q80TE7	Lrrc7	Leucine-rich repeat-containing protein 7	− 1.430	0.283	40.406
Q3UTJ2	Sorbs2	Sorbin and SH3 domain-containing protein 2	− 1.330	0.354	47.140
Q02257	Jup	Junction plakoglobin	− 1.330	0.354	47.140
P16546	Sptan1	Spectrin alpha chain, non-erythrocytic 1	− 1.240	0.318	39.371

The identified proteins are reported with their UniProt accession number (Acc#), gene and protein name, fold change (HI 1 h over sham) of relative levels of binding to GluN2B with the standard deviation (SD) and coefficient of variation (%CV). Calculation of fold change was made following IPA. If the association increased after HI, use values of (HI/sham), and if the association decreased after HI, use − 1(sham/HI).

involved in neurotransmitter release or synapse maintenance (Jaworski et al., 2009), was also induced after HI and showed elevated association with GluN2B. We have validated some of these interactions by co-IP experiments (Fig. 3) and the results were consistent with those from MS analysis. The interactions of PKC α, β, γ, CaMKII α, β and p38α with GluN2B sustained for at least 6 h ($p < 0.05$, $n = 5$–6), while Src-GluN2B binding was maintained elevated for 24 h. PKC, CaMKII and Src kinases are known to phosphorylate GluN2B at specific sites, and in a coordinated effort to modify NMDAR activity, localization/trafficking, conformation and the related signaling transduction (Chen and Roche, 2007; Salter et al., 2009).

3.4. Reduction of GluN2B-MAGUK protein interactions early after HI

The four MAGUK family members PSD95, PSD93, SAP102 and SAP97 are principal PSD scaffold proteins and well-characterized NMDAR binding partners (Niethammer et al., 1996). They were among the top proteins that have decreased interactions with GluN2B early (at 1 h) after HI (Table 2). This result was validated by co-IP experiments as shown in Fig. 4. The association between Glu2B and PSD95, PSD93 and SAP102 all reached the lowest levels at 1 h after HI ($p = 0.0034$ vs sham for PSD93 and PSD95; $p = 0.01$ vs sham for SAP102; $n = 6$), and gradually recovered over time. GluN2B-PSD95 interaction turned to be stronger than the sham animals at 6 h and 24 h post-HI ($p = 0.01$, $n = 6$).

3.5. Functional significance and disease association by IPA analysis

To determine whether the early responses of GluN2B complexes to neonatal HI predict activation or suppression of any biological processes and association of diseases, the protein data was interrogated with IPA and compared for different categories: (1) molecular and cellular functions, and (2) neurological disease and disorders. The top 10 hits for functional annotation and for neurological diseases and disorders annotations are listed in Table 3. Modification of the GluN2B signaling complexes early after HI mainly predicted reorganization of cytoplasm and cytoskeleton; release of neurotransmitter and neuroplasticity (LTP); increased microtubule dynamics and cell movement/migration and production of reactive oxygen species. Interestingly, organismal death was predicted to be inhibited at early reperfusion stage, possibly indicating a self-defense or protection mechanism acutely after the insult.

Changes in GluN2B complexes following neonatal HI are predicted to be associated with multiple neurological diseases and disorders. The IPA analysis did not provide the predicted activation status for any diseases except increased anxiety in the category of behavior, therefore, based on the *p*-values, the top 10 most significant diseases were listed. In addition to abnormal morphology of dendritic spines, neurons and nervous system; cell death of cerebral cortex cells, the alterations may predict HI-related neurological deficits, for example, disorder of basal ganglia, motor dysfunction or movement disorder.

4. Discussion

This study shows for the first time the protein composition of GluN2B-containing NMDAR complexes in the developing mouse brain and their modifications at early time points after neonatal HI. The GluN2B subunit was found to interact with 71 proteins localized at the PSD including mainly scaffold and cytoskeletal proteins. Within 24 h after hypoxia-ischemia, recruitment of multiple proteins into the complexes including various kinases, and the changes in GluN2B interactions with the existing partners suggest activation of new regulation mechanisms for NMDARs that may impact their function and downstream signaling pathways. These responses may also represent the earliest alterations of postsynaptic networks driven by activated NMDARs following HI.

The 71 native GluN2B-interacting proteins are classified into functional categories similar to those in the adult mouse brain (Bayes et al.,

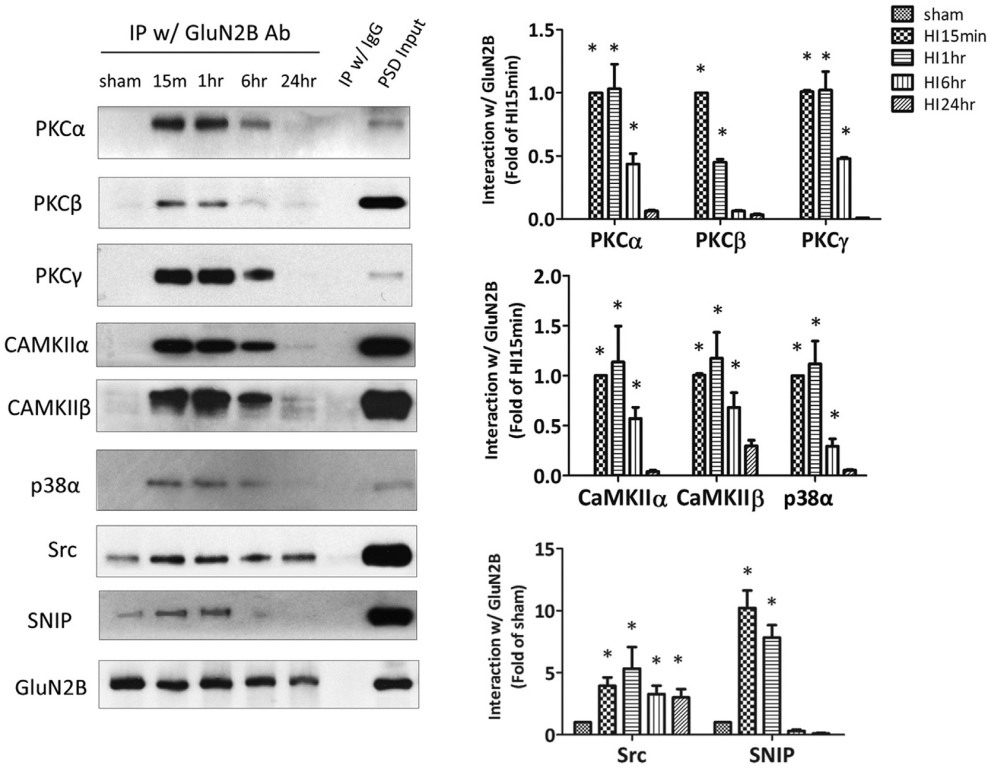

Fig. 3. Increased GluN2B interaction with multiple kinases after neonatal HI. IP with GluN2B antibody (Ab) followed by western blotting with the antibodies targeting the kinases shown on the left side of the blots. The levels of protein interaction are expressed as the OD ratio of co-IP'd protein (kinases) to GluN2B and normalized to the values at HI 15 min (for PKCα, β, γ, CaMKIIα, β and p38α) or the values of sham (for Src, SNIP). IP with mouse IgG served as negative control. (*$p < 0.05$ vs. sham, $n = 5–6$).

2012; Collins et al., 2006; Husi et al., 2000), among which 36 have been reported in the NMDAR complexes (NRC) and MAGUK-associated complexes (MASC) in the adult mouse brain. Half of them (35) are scaffold/adaptor and cytoskeletal/adhesion proteins, which form hierarchical structures to stabilize the receptors on the postsynaptic membranes and provide platforms for additional bindings with other PSD proteins. Unlike adult NRC/MASC, only a few signaling molecules, including three protein kinases (CaMKIIα, β and Src) are detected in the GluN2B complex. They are probably the master NMDAR kinases in the developing brain involved in the regulation of differential plasticity threshold of young synapses. Our previous proteomic study reported the presence of more kinases and several phosphatases in P9 cortex PSDs (Shao et al., 2017), without a side-by-side comparison with adult GluN2B complexes, it's not clear whether these kinases and phosphatases could interact with NMDAR at a later time to promote maturation of NMDAR signaling machinery and synapses.

Neonatal HI has a profound impact on the GluN2B complexes by recruiting new proteins into the complexes, and modifying the existing associations. MS has detected 37 proteins that are newly recruited to the complex 1 h after HI, binding to GluN2B directly or indirectly. These include the top four proteins (in Table 1) that showed increased expression at PSDs after HI, and peaked at the same time when their interactions with GluN2B reached the highest (Fig. 2). BRAG2, TANC2 and Eef1α1 have been reported to localize at PSDs and all play important roles in dendritic spine maturation and synapse development/activity, and therefore, are crucial for neurodevelopment and learning/memory (Elagabani et al., 2016; Han et al., 2010; Huang et al., 2005). For example, BRAG2 and the closely related BRAG1 (IQ motif and SEC7

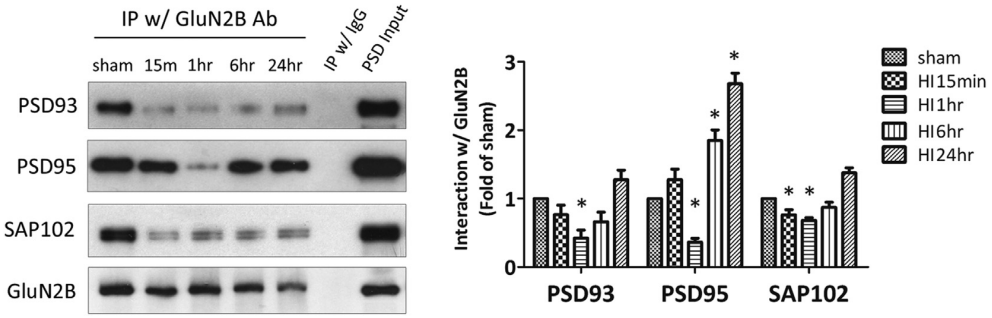

Fig. 4. Reduction of GluN2B-MAGUK protein interactions early after neonatal HI. IP with GluN2B antibody (Ab) followed by western blotting with the antibodies targeting the MAGUK proteins shown on the left side of the blots. The levels of protein interaction are expressed as the OD ratio of co-IP'd protein (PSD93, PSD95 or SAP102) to GluN2B and normalized to the sham values. IP with mouse IgG served as negative control. (*$p < 0.05$ vs. sham, $n = 5–6$).

Table 3
Diseases and functional annotations from GluN2B binding proteins after HI predicted by IPA.

Functional annotation	*p*-Value	# Molecules	Predicted activation
Organization of cytoplasm	3.21E-23	46	increased
Organization of cytoskeleton	6.62E-23	44	increased
Formation of cellular protrusions	1.31E-20	35	increased
Microtubule dynamics	1.25E-19	38	increased
Long-term potentiation	3.79E-12	15	increased
Release of neurotransmitter	2.28E-09	10	increased
Cell movement	3.13E-06	30	increased
Migration of cells	2.11E-04	24	increased
Production of reactive oxygen species	2.77E-03	7	increased
Phagocytosis of cells	3.23E-03	6	increased
Organismal death	1.08E-03	26	decreased
Neurological Disease annotation	***p*-Value**	**# Molecules**	**Predicted activation**
Anxiety	2.11E-11	13	increased
Abnormal morphology of nervous system	2.34E-08	19	
Motor dysfunction or movement disorder	1.89E-07	22	
Cell death of cerebral cortex cells	2.15E-07	10	
Abnormal morphology of neurons	2.22E-07	13	
Tauopathy	2.63E-07	16	
Movement Disorders	6.30E-07	21	
Alzheimer disease	9.03E-07	15	
Hyperesthesia	4.11E-06	7	
Abnormal morphology of dendritic spines	6.04E-06	4	
Disorder of basal ganglia	6.58E-06	16	

GluN2B-interacting proteins were analyzed by the Diseases and Bio Functions module in IPA. The reports were based on the proteins that were newly recruited to GluN2B complexes after HI and that showed increased or decreased interactions with GluN2B at 1 h after HI (85 proteins in total). *p* values reflect the significance of the association or overlap between proteins uploaded and a given function/disease. # Molecules are the number of proteins from the uploaded dataset that are associated with a given function/disease.

domain-containing protein 2, IQSEC2) are able to mediate calcium-dependent, subunit-specific functions of NMDAR through their physical binding with GluN2 C-terminus (Elagabani et al., 2016). BRAG1 was found to be associated with GluN2B in the naïve animals (Supplemental Table S1) at P9, in line with the recent report that NMDARs signal through GluN2B-BRAG1 during early development (Elagabani et al., 2016). Overexpression of BRAG2 at PSDs and/or increased interaction of BRAG2 with GluN2B after HI may impair GluN2B-BRAG1-mediated Arf6 activity and the related function in dendritic spine formation, development and maintenance; or may modify membrane trafficking/internalization of glutamate receptors (Scholz et al., 2010) and actin cytoskeleton (Hiroi et al., 2006).

TANC family proteins (TANC1 and TANC2) are considered as a postsynaptic scaffold as they associate with various PSD proteins including GluN2B (Suzuki et al., 2005). TANC2 is highly expressed in embryonic period till first 2–3 weeks after birth in rat brain and its synaptic localization is mediated by the direct PDZ domain interaction with PSD95 (Han et al., 2010). Overexpression of TANC2 in cultured neurons increases the density of spines and excitatory synapses that also requires its PSD95 interaction (Han et al., 2010). In our study, while barely detected in PSDs in sham animals, TANC2 underwent a rapid and robust translocation into PSDs and stayed there for at least 6 h. PSD95 may promote this translocation, although it's not clear whether PSD95-TANC2 binding was enhanced after HI and what the upstream regulators are for their interaction. GluN2B-TANC2 association after HI may expand the NMDAR networks as TANC2 could introduce additional interactions through its other domain structures (Suzuki et al., 2005). It's also possible that GluN2B and TANC2 compete for binding to PSD95 to modulate postsynaptic signaling after HI as GluN2B and TANC2 share the same PDZ binding motif for PSD95 (Bassand et al., 1999; Han et al., 2010; Kornau et al., 1995).

As expected, neonatal HI rapidly activates synaptic GluN2B phosphorylation networks (within 15 min and lasts at least 6–24 h). Besides the kinases that were validated by co-IP (CaMKIIα and β, PKCα, β and γ, p38α MAP kinase and Src kinase), reported GluN2B interactions in adult stroke or transient ischemia model, such as with death-associated protein kinase 1 (DAPK1) (Tu et al., 2010), with phosphoinositide 3-kinase (PI3K) subunit p85 (Takagi et al., 2003), were also enhanced early after HI (data not shown). These well-characterized kinases are capable of phosphorylating GluN2B at specific one or multiple sites. They might be part of the phosphorylation cascades activated after HI to amplify the original signal or crosstalk between different pathways. For example, PKC activation can trigger CaMKII autophosphorylation (Yan et al., 2011), or through Src family kinases (Cheung et al., 2003; Salter and Kalia, 2004), to regulate NMDAR function. Activation of NMDAR has been shown to change the phosphorylation status of 127 proteins (Coba et al., 2009). Switching on these kinase pathways is key for synaptic transduction at baseline, but aberrant activity or interactions after HI could rewrite the function of NMDAR and other substrates, being harmful to neural plasticity and associated learning and memory. On the other hand, increased kinase expression or interaction with GluN2B after HI could mediate NMDAR-dependent excitotoxic cell death, as reported with p38 MAP kinase (Fan et al., 2012; Soriano et al., 2008) and PKC (Wagey et al., 2001).

The MAGUK family proteins are central component of PSD and important for synaptic organization and plasticity. The reduced association of GluN2B with PSD95, PSD93 and SAP102 early after HI is possibly attributable to their decreased expression at the same time (Shao et al., 2017) except that SAP102 is down-regulated later at 6 h and afterwards. A recent triple-MAGUK (PSD95, PSD93 and SAP102) knockdown study demonstrated their critical roles in keeping AMPA and NMDA receptor complexes at the PSD and in maintaining the molecular organization of the PSDs (Chen et al., 2015). We observed roughly 50% reduction in PSD95 and PSD93 protein levels and their interactions with GluN2B early after HI. These changes may diminish the stability of both AMPA and NMDA receptors at PSDs and reduce synaptic transmission, or even result in smaller or loss of PSD. Furthermore, since the assembly of 1.5 MDa NMDAR super complexes after day 12 requires GluN2B, PSD95 and PSD93 (Frank et al., 2016), decreased levels of these proteins and their associations after neonatal HI might affect normal synapse maturation.

Depending on the nature of the injury and time when it occurs, either cortical gray matter and basal ganglia in the term newborn or subcortical white matter in the preterm are the primary lesion sites of hypoxic-ischemic encephalopathy (HIE) based on MRI imaging (Ferriero and Miller, 2010; Huang and Castillo, 2008; Merhar and Chau, 2016). Moderate to severe HIE are associated with poor clinical outcomes including motor impairment (dyskinetic cerebral palsy, epilepsy) and cognitive deficits (mental retardation and learning disability) (Ahearne et al., 2016; Pappas et al., 2015; Robertson and Perlman, 2006). The IPA analyses showed that the GluN2B-containing NMDAR complexes contain molecules involved in neurological diseases, including disorder of basal ganglia, motor dysfunction or movement disorder, in accordance with the different HIE clinical presentations. Although the role of NMDAR in dendritic spine morphology (Chen et al., 2011; Vastagh et al., 2012), learning/memory (Ten et al., 2003)

and anxiety (Barkus et al., 2010) has been substantiated in animal models; and GRIN2B mutation at CTD has implicated in Alzheimer disease (Hu et al., 2016), there is no current human data supporting the connection of HIE or NE with anxiety, tauopathy and Alzheimer disease. Furthermore, GluN2B CTD is known to initiate signaling cascades resulting in the production of both reactive oxygen and nitrogen species, such as superoxide (Brennan-Minnella et al., 2013) and nitric oxide (Girouard et al., 2009) that injury the neurons and their nearby cells (Reyes et al., 2012). This might be partly responsible for cell death of cerebral cortex cells (and other regions) and brain damage that was predicted by IPA.

5. Conclusions

Our study characterized the postsynaptic GluN2B interactome in the developing mouse brain, and their modifications early after neonatal HI. These data provide a resource for future studies of the molecular basis for developmental synaptic plasticity, and the mechanisms underlying neurological disorders and cognitive impairments in the conditions involving hypoxia-ischemia. Targeted disruption of specific GluN2B interaction is required to elucidate the functional consequence and contribution of specific pathway to HI-induced impairment of brain development. Since targeting the NMDAR alone interrupts their physiological function with serious side effects, identification of specific components of NMDAR pathway responsible for neuronal death will inform novel therapeutic approaches to selectively uncouple the NMDAR from harmful consequences while preserving their important beneficial functions in neonates.

Supplementary data to this article can be found online at https://doi.org/10.1016/j.expneurol.2017.10.005.

Acknowledgments

This work was supported by the National Institute of Neurological Disorders and Stroke (RO1NS084057 to Dr. Jiang). Mass Spectrometry was provided by the Bio-Organic Biomedical Mass Spectrometry Resource at UCSF (A.L. Burlingame, Director) supported by the Biomedical Technology Research Centers program of the National Institute of General Medical Sciences, NIH NIGMS 8P41GM103481.

References

Ahearne, C.E., Boylan, G.B., Murray, D.M., 2016. Short and long term prognosis in perinatal asphyxia: an update. World J. Clin. Pediatr. 5, 67–74.
Barkus, C., McHugh, S.B., Sprengel, R., Seeburg, P.H., Rawlins, J.N., Bannerman, D.M., 2010. Hippocampal NMDA receptors and anxiety: at the interface between cognition and emotion. Eur. J. Pharmacol. 626, 49–56.
Bassand, P., Bernard, A., Rafiki, A., Gayet, D., Khrestchatisky, M., 1999. Differential interaction of the tSXV motifs of the NR1 and NR2A NMDA receptor subunits with PSD-95 and SAP97. Eur. J. Neurosci. 11, 2031–2043.
Bayes, A., Collins, M.O., Croning, M.D., van de Lagemaat, L.N., Choudhary, J.S., Grant, S.G., 2012. Comparative study of human and mouse postsynaptic proteomes finds high compositional conservation and abundance differences for key synaptic proteins. PLoS One 7, e46683.
Bayes, A., Collins, M.O., Galtrey, C.M., Simonnet, C., Roy, M., Croning, M.D., Gou, G., van de Lagemaat, L.N., Milward, D., Whittle, I.R., Smith, C., Choudhary, J.S., Grant, S.G., 2014. Human post-mortem synapse proteome integrity screening for proteomic studies of postsynaptic complexes. Mol. Brain 7, 88.
Brennan-Minnella, A.M., Shen, Y., El-Benna, J., Swanson, R.A., 2013. Phosphoinositide 3-kinase couples NMDA receptors to superoxide release in excitotoxic neuronal death. Cell Death Dis. 4, e580.
Burnashev, N., Szepetowski, P., 2015. NMDA receptor subunit mutations in neurodevelopmental disorders. Curr. Opin. Pharmacol. 20, 73–82.
Chen, B.S., Roche, K.W., 2007. Regulation of NMDA receptors by phosphorylation. Neuropharmacology 53, 362–368.
Chen, B.S., Thomas, E.V., Sanz-Clemente, A., Roche, K.W., 2011. NMDA receptor-dependent regulation of dendritic spine morphology by SAP102 splice variants. J. Neurosci. 31, 89–96.
Chen, X., Levy, J.M., Hou, A., Winters, C., Azzam, R., Sousa, A.A., Leapman, R.D., Nicoll, R.A., Reese, T.S., 2015. PSD-95 family MAGUKs are essential for anchoring AMPA and NMDA receptor complexes at the postsynaptic density. Proc. Natl. Acad. Sci. U. S. A. 112, E6983–6992.
Cheung, H.H., Teves, L., Wallace, M.C., Gurd, J.W., 2003. Inhibition of protein kinase C reduces ischemia-induced tyrosine phosphorylation of the N-methyl-d-aspartate receptor. J. Neurochem. 86, 1441–1449.
Cho, S.J., Jung, J.S., Ko, B.H., Jin, I., Moon, I.S., 2004. Presence of translation elongation factor-1A (eEF1A) in the excitatory postsynaptic density of rat cerebral cortex. Neurosci. Lett. 366, 29–33.
Coba, M.P., Pocklington, A.J., Collins, M.O., Kopanitsa, M.V., Uren, R.T., Swamy, S., Croning, M.D., Choudhary, J.S., Grant, S.G., 2009. Neurotransmitters drive combinatorial multistate postsynaptic density networks. Sci. Signal. 2, ra19.
Collins, M.O., Husi, H., Yu, L., Brandon, J.M., Anderson, C.N., Blackstock, W.P., Choudhary, J.S., Grant, S.G., 2006. Molecular characterization and comparison of the components and multiprotein complexes in the postsynaptic proteome. J. Neurochem. 97 (Suppl. 1), 16–23.
de Vries, L.S., Jongmans, M.J., 2010. Long-term outcome after neonatal hypoxic-ischaemic encephalopathy. Arch. Dis. Child. Fetal Neonatal Ed. 95, F220–224.
Elagabani, M.N., Brisevac, D., Kintscher, M., Pohle, J., Kohr, G., Schmitz, D., Kornau, H.C., 2016. Subunit-selective N-methyl-d-aspartate (NMDA) receptor signaling through Brefeldin A-resistant Arf guanine nucleotide exchange factors BRAG1 and BRAG2 during synapse maturation. J. Biol. Chem. 291, 9105–9118.
Fan, J., Gladding, C.M., Wang, L., Zhang, L.Y., Kaufman, A.M., Milnerwood, A.J., Raymond, L.A., 2012. P38 MAPK is involved in enhanced NMDA receptor-dependent excitotoxicity in YAC transgenic mouse model of Huntington disease. Neurobiol. Dis. 45, 999–1009.
Fan, X., Jin, W.Y., Wang, Y.T., 2014. The NMDA receptor complex: a multifunctional machine at the glutamatergic synapse. Front. Cell. Neurosci. 8, 160.
Ferriero, D.M., Miller, S.P., 2010. Imaging selective vulnerability in the developing nervous system. J. Anat. 217, 429–435.
Frank, R.A., Komiyama, N.H., Ryan, T.J., Zhu, F., O'Dell, T.J., Grant, S.G., 2016. NMDA receptors are selectively partitioned into complexes and supercomplexes during synapse maturation. Nat. Commun. 7, 11264.
Girouard, H., Wang, G., Gallo, E.F., Anrather, J., Zhou, P., Pickel, V.M., Iadecola, C., 2009. NMDA receptor activation increases free radical production through nitric oxide and NOX2. J. Neurosci. 29, 2545–2552.
Giustetto, M., Hegde, A.N., Si, K., Casadio, A., Inokuchi, K., Pei, W., Kandel, E.R., Schwartz, J.H., 2003. Axonal transport of eukaryotic translation elongation factor 1alpha mRNA couples transcription in the nucleus to long-term facilitation at the synapse. Proc. Natl. Acad. Sci. U. S. A. 100, 13680–13685.
Hall, B.J., Ripley, B., Ghosh, A., 2007. NR2B signaling regulates the development of synaptic AMPA receptor current. J. Neurosci. 27, 13446–13456.
Han, S., Nam, J., Li, Y., Kim, S., Cho, S.H., Cho, Y.S., Choi, S.Y., Choi, J., Han, K., Kim, Y., Na, M., Kim, H., Bae, Y.C., Choi, S.Y., Kim, E., 2010. Regulation of dendritic spines, spatial memory, and embryonic development by the TANC family of PSD-95-interacting proteins. J. Neurosci. 30, 15102–15112.
Hansen, H.H., Briem, T., Dzietko, M., Sifringer, M., Voss, A., Rzeski, W., Zdzisinska, B., Thor, F., Heumann, R., Stepulak, A., Bittigau, P., Ikonomidou, C., 2004. Mechanisms leading to disseminated apoptosis following NMDA receptor blockade in the developing rat brain. Neurobiol. Dis. 16, 440–453.
Hill, W.D., Davies, G., van de Lagemaat, L.N., Christoforou, A., Marioni, R.E., Fernandes, C.P., Liewald, D.C., Croning, M.D., Payton, A., Craig, L.C., Whalley, L.J., Horan, M., Ollier, W., Hansell, N.K., Wright, M.J., Martin, N.G., Montgomery, G.W., Steen, V.M., Le Hellard, S., Espeseth, T., Lundervold, A.J., Reinvang, I., Starr, J.M., Pendleton, N., Grant, S.G., Bates, T.C., Deary, I.J., 2014. Human cognitive ability is influenced by genetic variation in components of postsynaptic signalling complexes assembled by NMDA receptors and MAGUK proteins. Transl. Psychiatry 4, e341.
Hiroi, T., Someya, A., Thompson, W., Moss, J., Vaughan, M., 2006. GEP100/BRAG2: activator of ADP-ribosylation factor 6 for regulation of cell adhesion and actin cytoskeleton via E-cadherin and alpha-catenin. Proc. Natl. Acad. Sci. U. S. A. 103, 10672–10677.
Hu, C., Chen, W., Myers, S.J., Yuan, H., Traynelis, S.F., 2016. Human GRIN2B variants in neurodevelopmental disorders. J. Pharmacol. Sci. 132, 115–121.
Huang, B.Y., Castillo, M., 2008. Hypoxic-ischemic brain injury: imaging findings from birth to adulthood. Radiographics 28, 417–439 (quiz 617).
Huang, F., Chotiner, J.K., Steward, O., 2005. The mRNA for elongation factor 1alpha is localized in dendrites and translated in response to treatments that induce long-term depression. J. Neurosci. 25, 7199–7209.
Husi, H., Grant, S.G., 2001. Isolation of 2000-kDa complexes of N-methyl-D-aspartate receptor and postsynaptic density 95 from mouse brain. J. Neurochem. 77, 281–291.
Husi, H., Ward, M.A., Choudhary, J.S., Blackstock, W.P., Grant, S.G., 2000. Proteomic analysis of NMDA receptor-adhesion protein signaling complexes. Nat. Neurosci. 3, 661–669.
Jaworski, J., Kapitein, L.C., Gouveia, S.M., Dortland, B.R., Wulf, P.S., Grigoriev, I., Camera, P., Spangler, S.A., Di Stefano, P., Demmers, J., Krugers, H., Defilippi, P., Akhmanova, A., Hoogenraad, C.C., 2009. Dynamic microtubules regulate dendritic spine morphology and synaptic plasticity. Neuron 61, 85–100.
Jiang, X., Mu, D., Manabat, C., Koshy, A.A., Christen, S., Tauber, M.G., Vexler, Z.S., Ferriero, D.M., 2004. Differential vulnerability of immature murine neurons to oxygen-glucose deprivation. Exp. Neurol. 190, 224–232.
Jiang, X., Knox, R., Pathipati, P., Ferriero, D., 2011. Developmental localization of NMDA receptors, Src and MAP kinases in mouse brain. Neurosci. Lett. 503, 215–219.
Kim, S., Pevzner, P.A., 2014. MS-GF + makes progress towards a universal database search tool for proteomics. Nat. Commun. 5, 5277.
Knox, R., Zhao, C., Miguel-Perez, D., Wang, S., Yuan, J., Ferriero, D., Jiang, X., 2013. Enhanced NMDA receptor tyrosine phosphorylation and increased brain injury following neonatal hypoxia-ischemia in mice with neuronal Fyn overexpression. Neurobiol. Dis. 51, 113–119.
Kornau, H.C., Schenker, L.T., Kennedy, M.B., Seeburg, P.H., 1995. Domain interaction between NMDA receptor subunits and the postsynaptic density protein PSD-95.

Science 269, 1737–1740.
Kutsuwada, T., Sakimura, K., Manabe, T., Takayama, C., Katakura, N., Kushiya, E., Natsume, R., Watanabe, M., Inoue, Y., Yagi, T., Aizawa, S., Arakawa, M., Takahashi, T., Nakamura, Y., Mori, H., Mishina, M., 1996. Impairment of suckling response, trigeminal neuronal pattern formation, and hippocampal LTD in NMDA receptor epsilon 2 subunit mutant mice. Neuron 16, 333–344.
Mancini, J.D., Atchison, W.D., 2007. The NR2B subunit in NMDA receptors is functionally important during cerebellar granule cell migration. Neurosci. Lett. 429, 87–90.
Martel, M.A., Ryan, T.J., Bell, K.F., Fowler, J.H., McMahon, A., Al-Mubarak, B., Komiyama, N.H., Horsburgh, K., Kind, P.C., Grant, S.G., Wyllie, D.J., Hardingham, G.E., 2012. The subtype of GluN2 C-terminal domain determines the response to excitotoxic insults. Neuron 74, 543–556.
Martinez-Lopez, M.J., Alcantara, S., Mascaro, C., Perez-Branguli, F., Ruiz-Lozano, P., Maes, T., Soriano, E., Buesa, C., 2005. Mouse neuron navigator 1, a novel microtubule-associated protein involved in neuronal migration. Mol. Cell. Neurosci. 28, 599–612.
Merhar, S.L., Chau, V., 2016. Neuroimaging and other neurodiagnostic tests in neonatal encephalopathy. Clin. Perinatol. 43, 511–527.
Millar, L.J., Shi, L., Hoerder-Suabedissen, A., Molnar, Z., 2017. Neonatal hypoxia ischaemia: mechanisms, models, and therapeutic challenges. Front. Cell. Neurosci. 11, 78.
Monyer, H., Burnashev, N., Laurie, D.J., Sakmann, B., Seeburg, P.H., 1994. Developmental and regional expression in the rat brain and functional properties of four NMDA receptors. Neuron 12, 529–540.
Niethammer, M., Kim, E., Sheng, M., 1996. Interaction between the C terminus of NMDA receptor subunits and multiple members of the PSD-95 family of membrane-associated guanylate kinases. J. Neurosci. 16, 2157–2163.
Ohno, T., Maeda, H., Murabe, N., Kamiyama, T., Yoshioka, N., Mishina, M., Sakurai, M., 2010. Specific involvement of postsynaptic GluN2B-containing NMDA receptors in the developmental elimination of corticospinal synapses. Proc. Natl. Acad. Sci. U. S. A. 107, 15252–15257.
Old, W.M., Meyer-Arendt, K., Aveline-Wolf, L., Pierce, K.G., Mendoza, A., Sevinsky, J.R., Resing, K.A., Ahn, N.G., 2005. Comparison of label-free methods for quantifying human proteins by shotgun proteomics. Mol. Cell. Proteomics 4, 1487–1502.
Paoletti, P., Bellone, C., Zhou, Q., 2013. NMDA receptor subunit diversity: impact on receptor properties, synaptic plasticity and disease. Nat. Rev. Neurosci. 14, 383–400.
Pappas, A., Shankaran, S., McDonald, S.A., Vohr, B.R., Hintz, S.R., Ehrenkranz, R.A., Tyson, J.E., Yolton, K., Das, A., Bara, R., Hammond, J., Higgins, R.D., Hypothermia Extended Follow-up Subcommittee of the Eunice Kennedy Shriver, N.N.R.N, 2015. Cognitive outcomes after neonatal encephalopathy. Pediatrics 135, e624–634.
Perez, A., Ritter, S., Brotschi, B., Werner, H., Caflisch, J., Martin, E., Latal, B., 2013. Long-term neurodevelopmental outcome with hypoxic-ischemic encephalopathy. J. Pediatr. 163, 454–459.
Pocklington, A.J., Cumiskey, M., Armstrong, J.D., Grant, S.G., 2006. The proteomes of neurotransmitter receptor complexes form modular networks with distributed functionality underlying plasticity and behaviour. Mol. Syst. Biol. 2 (2006), 0023.
Reyes, R.C., Brennan, A.M., Shen, Y., Baldwin, Y., Swanson, R.A., 2012. Activation of neuronal NMDA receptors induces superoxide-mediated oxidative stress in neighboring neurons and astrocytes. J. Neurosci. 32, 12973–12978.
Rice 3rd, J.E., Vannucci, R.C., Brierley, J.B., 1981. The influence of immaturity on hypoxic-ischemic brain damage in the rat. Ann. Neurol. 9, 131–141.
Robertson, C.M., Perlman, M., 2006. Follow-up of the term infant after hypoxic-ischemic encephalopathy. Paediatr. Child Health 11, 278–282.
Salter, M.W., Kalia, L.V., 2004. Src kinases: a hub for NMDA receptor regulation. Nat. Rev. Neurosci. 5, 317–328.
Salter, M.W., Dong, Y., Kalia, L.V., Liu, X.J., Pitcher, G., 2009. Regulation of NMDA receptors by kinases and phosphatases. In: Van Dongen, A.M. (Ed.), Biology of the NMDA Receptor, (Boca Raton (FL)).
Scholz, R., Berberich, S., Rathgeber, L., Kolleker, A., Kohr, G., Kornau, H.C., 2010. AMPA receptor signaling through BRAG2 and Arf6 critical for long-term synaptic depression. Neuron 66, 768–780.
Shao, G., Wang, Y., Guan, S., Burlingame, A.L., Lu, F., Knox, R., Ferriero, D.M., Jiang, X., 2017. Proteomic analysis of mouse cortex postsynaptic density following neonatal brain hypoxia-ischemia. Dev. Neurosci. 39, 66–81.
Shu, S., Pei, L., Lu, Y., 2014. Promising targets of cell death signaling of NR2B receptor subunit in stroke pathogenesis. Regen. Med. Res. 2, 8.
Soriano, F.X., Martel, M.A., Papadia, S., Vaslin, A., Baxter, P., Rickman, C., Forder, J., Tymianski, M., Duncan, R., Aarts, M., Clarke, P., Wyllie, D.J., Hardingham, G.E., 2008. Specific targeting of pro-death NMDA receptor signals with differing reliance on the NR2B PDZ ligand. J. Neurosci. 28, 10696–10710.
Sprengel, R., Suchanek, B., Amico, C., Brusa, R., Burnashev, N., Rozov, A., Hvalby, O., Jensen, V., Paulsen, O., Andersen, P., Kim, J.J., Thompson, R.F., Sun, W., Webster, L.C., Grant, S.G., Eilers, J., Konnerth, A., Li, J., McNamara, J.O., Seeburg, P.H., 1998. Importance of the intracellular domain of NR2 subunits for NMDA receptor function in vivo. Cell 92, 279–289.
Sun, Y., Zhang, L., Chen, Y., Zhan, L., Gao, Z., 2015. Therapeutic targets for cerebral ischemia based on the signaling pathways of the GluN2B C terminus. Stroke 46, 2347–2353.
Suzuki, T., Li, W., Zhang, J.P., Tian, Q.B., Sakagami, H., Usuda, N., Kondo, H., Fujii, T., Endo, S., 2005. A novel scaffold protein, TANC, possibly a rat homolog of drosophila rolling pebbles (rols), forms a multiprotein complex with various postsynaptic density proteins. Eur. J. Neurosci. 21, 339–350.
Takagi, N., Sasakawa, K., Besshoh, S., Miyake-Takagi, K., Takeo, S., 2003. Transient ischemia enhances tyrosine phosphorylation and binding of the NMDA receptor to the Src homology 2 domain of phosphatidylinositol 3-kinase in the rat hippocampus. J. Neurochem. 84, 67–76.
Tarnok, K., Czondor, K., Jelitai, M., Czirok, A., Schlett, K., 2008. NMDA receptor NR2B subunit over-expression increases cerebellar granule cell migratory activity. J. Neurochem. 104, 818–829.
Ten, V.S., Bradley-Moore, M., Gingrich, J.A., Stark, R.I., Pinsky, D.J., 2003. Brain injury and neurofunctional deficit in neonatal mice with hypoxic-ischemic encephalopathy. Behav. Brain Res. 145, 209–219.
Tu, W., Xu, X., Peng, L., Zhong, X., Zhang, W., Soundarapandian, M.M., Balel, C., Wang, M., Jia, N., Zhang, W., Lew, F., Chan, S.L., Chen, Y., Lu, Y., 2010. DAPK1 interaction with NMDA receptor NR2B subunits mediates brain damage in stroke. Cell 140, 222–234.
Um, J.W., 2017. Synaptic functions of the IQSEC family of ADP-ribosylation factor guanine nucleotide exchange factors. Neurosci. Res. 116, 54–59.
van Handel, M., Swaab, H., de Vries, L.S., Jongmans, M.J., 2007. Long-term cognitive and behavioral consequences of neonatal encephalopathy following perinatal asphyxia: a review. Eur. J. Pediatr. 166, 645–654.
Vastagh, C., Gardoni, F., Bagetta, V., Stanic, J., Zianni, E., Giampa, C., Picconi, B., Calabresi, P., Di Luca, M., 2012. N-methyl-D-aspartate (NMDA) receptor composition modulates dendritic spine morphology in striatal medium spiny neurons. J. Biol. Chem. 287, 18103–18114.
Wagey, R., Hu, J., Pelech, S.L., Raymond, L.A., Krieger, C., 2001. Modulation of NMDA-mediated excitotoxicity by protein kinase C. J. Neurochem. 78, 715–726.
Wang, C.C., Held, R.G., Chang, S.C., Yang, L., Delpire, E., Ghosh, A., Hall, B.J., 2011. A critical role for GluN2B-containing NMDA receptors in cortical development and function. Neuron 72, 789–805.
Wenzel, A., Fritschy, J.M., Mohler, H., Benke, D., 1997. NMDA receptor heterogeneity during postnatal development of the rat brain: differential expression of the NR2A, NR2B, and NR2C subunit proteins. J. Neurochem. 68, 469–478.
Yan, J.Z., Xu, Z., Ren, S.Q., Hu, B., Yao, W., Wang, S.H., Liu, S.Y., Lu, W., 2011. Protein kinase C promotes N-methyl-D-aspartate (NMDA) receptor trafficking by indirectly triggering calcium/calmodulin-dependent protein kinase II (CaMKII) autophosphorylation. J. Biol. Chem. 286, 25187–25200.